Mitochondrial Topoisomerase I Sites in the Regulatory D-Loop Region of Mitochondrial DNA[†]

Hongliang Zhang and Yves Pommier*

Laboratory of Molecular Pharmacology, Center for Cancer Research, National Cancer Institute, National Institutes of Health, Bethesda, Maryland 20892-4255

ABSTRACT: Mitochondrial DNA (mtDNA) is required for mitochondrial activities because it encodes key proteins for oxidative phosphorylation and the production of cellular ATP. We previously reported the existence of a specific mitochondrial topoisomerase gene, Top1mt, in all vertebrates. The corresponding polypeptide contains an N-terminal mitochondrial targeting sequence and is otherwise highly homologous to the nuclear topoisomerase I (Top1). In this study, we provide biochemical evidence of the presence of an endogenous Top1mt polypeptide in human mitochondria. Using novel antibodies against Top1mt, we detected the corresponding 70 kDa polypeptide in mitochondria but not in nuclear fractions. This polypeptide could be trapped to form covalent complexes with mtDNA when mitochondria from human cells were treated with camptothecin. Mapping of Top1mt sites in the regulatory D-loop region of mtDNA in mitochondria revealed the presence of an asymmetric cluster of Top1mt sites confined to a 150 bp segment downstream from, and adjacent to, the site at which replication is prematurely terminated, generating an ≈650-base (7S DNA) product that forms the mitochondrial D-loop. Moreover, we show that inhibition of Top1mt by camptothecin reduces the level of formation of the 7S DNA. These results suggest novel roles for Top1mt in regulating mtDNA replication.

Somatic cells contain thousands of copies of mitochondrial DNA (mtDNA),[1] which consist of duplex DNA circles encoding genes essential for oxidative phosphorylation and cellular metabolism. mtDNA replication must, therefore, be tightly controlled. Defects in mtDNA result in mitochondrial diseases, including neurological degeneration, ataxia, heart failure, diabetes, aging, and cancers (1−4). mtDNA represents 1−5% of the total cellular DNA content (5). Typically, mtDNA consists of 16569 bp circles containing intron-less genes. Mitochondrial genes are compactly arranged on both DNA strands (the H- and L-strands) and encode two rRNAs, 13 proteins implicated in oxidative phosphorylation, and 22 tRNAs (6, 7) (www.mitomap.org).

The regulatory region for mtDNA transcription and replication consists of a 1.3 kb noncoding region flanked by the three promoters (HSP1, HSP2, and LSP) and the transcription termination region for the H-strand (see Figures 3B and 8). It also includes the origin of replication. In animal mtDNA replication, most nascent strands from the leading, heavy-strand origin (O_H) are prematurely terminated, generating a 650-base, 7S DNA product that defines the 3′ boundary of the so-called "displacement loop" (D-loop). Proper formation of the D-loop is critical to the entire replication process and therefore to the integrity of the cell,

but the control elements for it have not been identified (8, 9). In cells, mtDNA is packaged in protein−DNA complexes named nucleoids (10) that are attached to the inner mitochondrial membrane by the mtDNA regulatory region (11).

The proteins required for mtDNA transcription, replication, repair, and nucleoid structure are all encoded in the nuclear genome and imported into mitochondria (7). Just like for any other DNA, mtDNA needs DNA topoisomerases for transcription and replication. Topoisomerases use DNA strand scission and rejoining activities to adjust DNA topology. They are classified into two categories. Type I enzymes transiently break one DNA strand at a time, whereas type II enzymes cleave and religate both strands of the DNA double helix in concert (12, 13). Human cells contain two type IA topoisomerases (Top3α and Top3β), two type IB topoisomerases (Top1 and Top1mt) (14, 15), and two type IIA topoisomerases (Top2α and Top2β) (13, 16). Topoisomerase activities have been identified in mitochondria from many species and tissues (15, 17−19). Because of the minute amount of mitochondrial topoisomerase activity compared with those of their nuclear counterparts, attempts to identify mitochondrial topoisomerases have been largely unsuccessful until the discovery of a specific mitochondrial DNA topoisomerase gene from human cells, Top1mt (20).

Top1mt, like its nuclear counterpart Top1, consists of four domains: an N-terminal localization domain, a core domain, a linker domain, and a C-terminal domain containing the catalytic tyrosine (15, 20, 21). The N-terminal domain of Top1mt is short (50 amino acid residues) and consists primarily of a mitochondrial localization signal. By contrast, the N-terminal domain of (nuclear) Top1 consists of 214

[1] Abbreviations: CPT, camptothecin; mtDNA, mitochondrial DNA; Top, topoisomerase; Top1, topoisomerase I; Top1mt, mitochondrial topoisomerase I.

Table 1: Primer Sets for PL-PCR (see Figures 2−5, 8, and 9)

primer name	sequence (from 5′ to 3′)	length	T_m (°C)
HP1.1	TTTCAGTGTATTGCTTTGAGGAGG	24mer	59.3
HP1.2	GAGGAGGTAAGCTACATAAACTGTGGG	27mer	65.0
HP1.3	GTAAGCTACATAAACTGTGGGGGGTGTC	28mer	66.6
HP2.1	GTTATGATGTCTGTGTGGAAAGCG	24mer	61.0
HP2.2	ATGTCTGTGTGGAAAGCGGCTGTG	24mer	64.4
HP2.3	GTGGAAAGCGGCTGTGCAGACATTC	25mer	66.3
HP3.1	CGGTAAATGGCTTTATGTGCTATG	24mer	59.3
HP3.2	GGGTGGGTAGGTTTGTTGGTATCCTAG	27mer	66.5
HP3.3	GGGTAGGTTTGTTGGTATCCTAGTGGGTG	29mer	68.1
LP2.1	CTGTTCTTTCATGGGGAAGCAG	22mer	60.3
LP2.2	GAAGCAGATTTGGGTACCACCCAAG	25mer	64.6
LP2.3	GGGTACCACCCAAGTATTGACTCACCC	27mer	68.0
LP3.1	GACTCCTAGCCGCAGACCTC	20mer	59.6
LP3.2	CTGAATCGGAGGACAACCAGTAAGC	25mer	64.6
LP3.3	GAATCGGAGGACAACCAGTAAGCTACCC	28mer	68.0
HM15643	GTTTATGACTGTATGGTGTATGTCAG	26mer	60.1
HM15637	GACTGTATGGTGTATGTCAGATAACACAG	29mer	63.9
phosphate linker (PL)	p-GAATTCAGATCTCCCGGGTCACCGC		
complementary linker	GATCTGAATTC-dd (2′,3′-dideoxy C)		
linker primer (LP)	GCGGTGACCCGGGAGATCTGAATTC		

amino acid residues encoding nuclear localization signals and protein−protein interaction motifs (*13*). The core and C-terminal domains and, to a lesser extent, the linker domain are highly similar between Top1mt and Top1 (*15*). These three domains are sufficient for topoisomerase activities and are encoded by 13 conserved exons. The 13-exon motif is conserved in all vertebrate type IB topoisomerase genes (*21*). Both Top1 (nuclear) and recombinant Top1mt can be trapped by camptothecin (CPT) (*20, 22*), a plant alkaloid highly selective for Top1, and from which two derivatives (topotecan and irinotecan) for treating human cancers have been derived (*14*).

Here we demonstrate the association of Top1mt with mtDNA using novel anti-Top1mt antibodies. We mapped the Top1mt sites induced by CPT in the regulatory D-loop region of mtDNA and show their asymmetrical localization downstream from the D-loop in mitochondria, whereas the Top1mt sites exhibited a more diffuse distribution when recombinant Top1mt was incubated with purified mtDNA. We also show that Top1mt inhibition by CPT affects formation of the 7S DNA associated with regulatory D-loops.

MATERIALS AND METHODS

Top1mt Antibodies. Top1mt protein was overexpressed using the pET system (Novagen, Madison, WI) (*20*). His-tagged Top1mt was purified and injected into rabbits (Spring Valley Laboratories, Woodbine, MD). The antiserum was affinity-purified using GST-tagged Top1mt.

Preparation of Mitochondria. Human breast cancer MCF-7 cells were washed with ice-cold phosphate-buffered saline (PBS), scrapped off, and spun down at 500*g* for 5 min. Mitochondrial preparation was performed as described previously (*23*). Briefly, cell pellets were resuspended in CaRSB buffer [10 mM NaCl, 1.5 mM CaCl₂, and 10 mM Tris-HCl (pH 7.5) at 25 °C] for 5 min. Following osmotic shock, cells were homogenized using a glass Dounce homogenizer (35 strokes). One-sixth volume of stabilizing buffer [2 M sucrose, 35 mM EDTA, and 50 mM Tris-HCl (pH 7.5) at 25 °C] was added to the cell lysates and mixed with two additional strokes with a glass Dounce homogenizer. Cell lysates were centrifuged at 750*g* for 5 min to remove the nuclei and cell

debris. Supernatants were collected, and the previous step was repeated once more. The mitochondria were spun down from the supernatant at 10000*g* for 20 min, washed with MT buffer [250 mM sucrose, 10 mM KCl, 1.5 mM MgCl₂, 1 mM EDTA, 1 mM EGTA, 5 mM DTT, and 20 mM Hepes-KOH (pH 7.4) at 25 °C], and resuspended in MT buffer.

Preparation of mtDNA. Mitochondria in MT buffer were lysed by adding sodium dodecyl sulfate (SDS) to a final concentration of 0.6% and proteinase K (0.1 mg/mL). The remaining steps followed the manufacturer's protocol for the DNeasy tissue kit (Qiagen, Valencia, CA).

Detection of Top1mt Cleavage Complexes Using the ICE Bioassay. The in vivo complex of enzyme (ICE) bioassays were performed as described previously (*24, 25*). Mitochondria were lysed with 1% sarkosyl and gently loaded on top of a CsCl gradient. After ultracentrifugation (Beckman SW40 rotor at 30700 rpm for 20 h at 20 °C), the samples were collected from the bottom of the centrifuge tubes and transferred to the Imobilon P membrane (Millipore, Bedford, MA). Top1mt was detected using a standard Western blotting protocol.

Phosphate-Linked Ligation-Mediated PCR (PL-PCR). The PL-PCR method was derived from the LM-PCR method previously used to map the DNA cleavage sites of nuclear Top1 in human rDNA (*26, 27*). To map the cleavage complexes produced by Top1mt in mtDNA, three primers were used in each set of experiments (Figure 3 and Table 1). The first primer was used to create the substrate for the phosphate linker (step a, Figure 3). The second primer was for PCR amplification (step c, Figure 3), and the third one was for labeling the PCR product to generate detectable signals (step d, Figure 3). Briefly, primer 1 was mixed with DNA samples in first strand buffer [40 mM NaCl, 10 mM Tris-HCl (pH 8.9) at 25 °C, 5 mM MgSO₄, 0.01% gelatin, and 250 µM dNTP] with Vent DNA polymerase (NEB, Beverly, MA) (step a, Figure 3). Incubation cycles were as follows: 95 °C for 5 min, 60 °C for 30 min, and 76 °C for 10 min (step a, Figure 3). The ligase dilution solution [110 mM Tris-HCl (pH 7.5) at 25 °C, 17.5 mM MgCl₂, 50 mM DTT, and 125 µg/mL BSA] and annealed phosphate linker were added, and ligation was carried out with T4 DNA ligase at 17 °C overnight (step b, Figure 3). The ligation mixture

was precipitated, dissolved in H$_2$O, and used as the PCR template. PCR was carried out with primer 2 and the linker primer (step c, Figure 3). The PCR conditions were as follows: step 1, one cycle at 95 °C for 3 min; step 2, 20 cycles consisting of 95 °C for 1 min, 66 °C for 2 min, and 76 °C for 3 min; step 3, one cycle at 76 °C for 10 min. The ^{32}P-labeled primer 3 was added to the PCR solutions, and the tubes were further incubated at 95 °C for 4 min, 70 °C for 2 min, 76 °C for 3 min, 95 °C for 1 min, 70 °C for 2 min, and 76 °C for 10 min (step d, Figure 3). The final solution was mixed with an equal volume of 2× loading buffer and directly loaded on 6% PAGE−urea gels.

In Vitro Top1mt Cleavage Assay. Double-stranded mtDNA fragments and oligonucleotides were 3′-end-labeled with ^{32}P. Labeled DNA (50 fmol/reaction) was incubated with 50 ng of recombinant Top1mt (*20*) with or without drug at 37 °C for 10 min in 10 µL of reaction buffer [10 mM Tris-HCl (pH 8.5), 50 mM KCl, 5 mM MgCl$_2$, 0.1 mM EDTA, and 15 µg/mL BSA, final concentrations]. Maxam−Gilbert loading buffer was added to the reaction mixtures. Aliquots were separated in denaturing polyacrylamide gels (7 M urea) in 1× TBE. Imaging and quantitation were performed using a PhosphorImager (Molecular Dynamics, Sunnyvale, CA).

Mapping the 3′ End of 7S DNA Associated with the mtDNA D-Loop. A modified version of PL-PCR was used. DNA samples were directly ligated with annealed phosphate linker by T4 DNA ligase at 17 °C overnight. After ligation, the protocol followed steps c and d of PL-PCR (see Figure 3). The primers used for PCR were LP and HM15643 for mouse and LP and HP3.2 for human mitochondria (see Table 1). Labeling and sequencing were performed after extension of the ^{32}P-5′-end-labeled HM15637 and HP3.3 nested primer for mouse and human mitochondria, respectively (see Table 1).

Generation of the Top1mt$^{-/-}$ MEF Cell Lines. The Top1mt$^{-/-}$ MEF cells were generated from Top1mt$^{-/-}$ mice, which were created by deletion of the last two exons of the Top1mt gene (*21*).

RESULTS

Top1mt Antibodies Demonstrate the Presence of Top1mt in Mitochondria. In spite of the high degree of homology between Top1mt and Top1 (nuclear) (*20*), Western blotting of mitochondrial lysates with available polyclonal and monoclonal antibodies against Top1 (nuclear) failed to detect a band with the expected size for Top1mt (Figure 1 and additional data not shown) even when the mitochondrial lysates exhibited a strong signal for Cox4 [a well-established mitochondrial polypeptide (data not shown)]. Thus, we generated anti-Top1mt polyclonal antibodies using recombinant full-length Top1mt to immunize rabbits. Those antibodies recognize a band of ≈70 kDa in mitochondrial lysates (Figure 1, lane M). That size is in agreement with the predicted molecular mass of Top1mt (69.9 kDa for the 601-amino acid polypeptide analyzed with MacVector). Our Top1mt antibodies also recognized nuclear Top1 (Figure 1, lane N). Those experiments indicate the presence of Top1mt in mitochondria. The lack of signal for Top1 (nuclear) in the mitochondrial fractions also demonstrates the absence of nuclear contamination in our mitochondrial preparations.
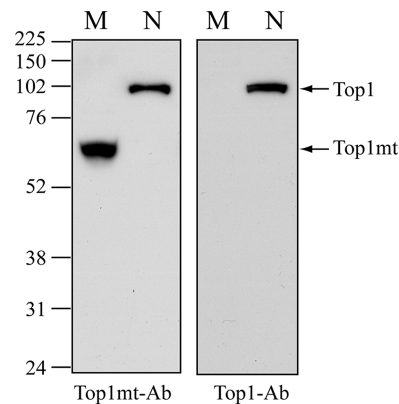
FIGURE 1: Detection of Top1mt in mitochondria by immunoblotting. The left panel shows Western blotting with Top1mt antibodies (Top1mt-Ab); the right panel shows the same membrane striped and reprobed with monoclonal Top1-Ab (Top1-Ab; C21): lane M, mitochondrial fraction; lane N, nuclear fraction. The migration positions of protein markers (kilodaltons) are indicated at the left.
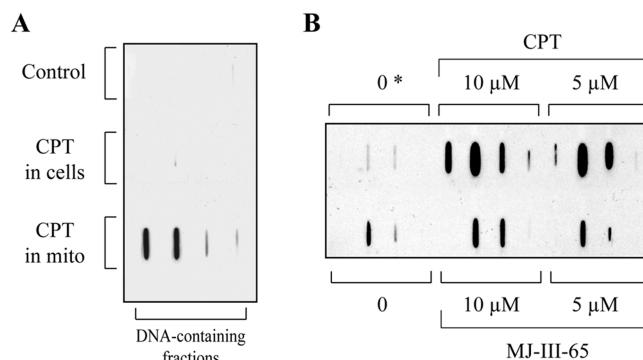
FIGURE 2: Induction of Top1mt−DNA complexes by CPT and the indenoisoquinoline (MJ-III-65, NSC 706744) in mitochondria from human breast cancer MCF-7 cells. (A) Detection of Top1mt−DNA complexes in cells vs mitochondria. Control: untreated cells. CPT in cells: cells treated with 5 µM CPT for 1 h at 37 °C before mitochondria were purified in the absence of CPT. CPT in mito: mitochondria isolated from untreated cells were treated with 5 µM CPT for 30 min at 37 °C. (B) Induction of Top1mt−DNA complexes in isolated mitochondria. Mitochondria were treated with the indicated drug concentrations for 30 min at 37 °C as indicated. Two control untreated samples are included: 0, sample without drug for 30 min at 37 °C; 0*, untreated sample kept on ice for 30 min while the other samples were incubated at 37 °C.

Trapping of Top1mt by Camptothecin in Mitochondria. To reveal interaction of Top1mt with mtDNA, we took advantage of the fact that Top1mt cleavage complexes can be trapped specifically by CPT (*20*) and that Top1 cleavage complexes can be visualized using Top1 antibodies following isolation of DNA by cesium gradient centrifugation (*24, 25*). Having generated the antibodies that recognize Top1mt (see above), we were able to look for the presence of Top1mt cleavage complexes in mitochondria treated with CPT. Figure 2 shows that treatment of cells with a relatively high dose of CPT (5 µM for 1 h) that are known to produce high levels of cleavage complexes with nuclear Top1 (*26−28*) failed to produce detectable Top1mt−DNA complexes (Figure 2A). However, treatment of isolated mitochondria with CPT for a half-hour generated Top1mt−mtDNA complexes (Figure 2). Topotecan, a clinical CPT derivative, was as effective as CPT (data not shown). We also tested the non-camptothecin indenoisoquinoline Top1 inhibitor, MJ-III-65 (NSC 706744) (*29*). MJ-III-65 also produced Top1mt−mtDNA cleavage
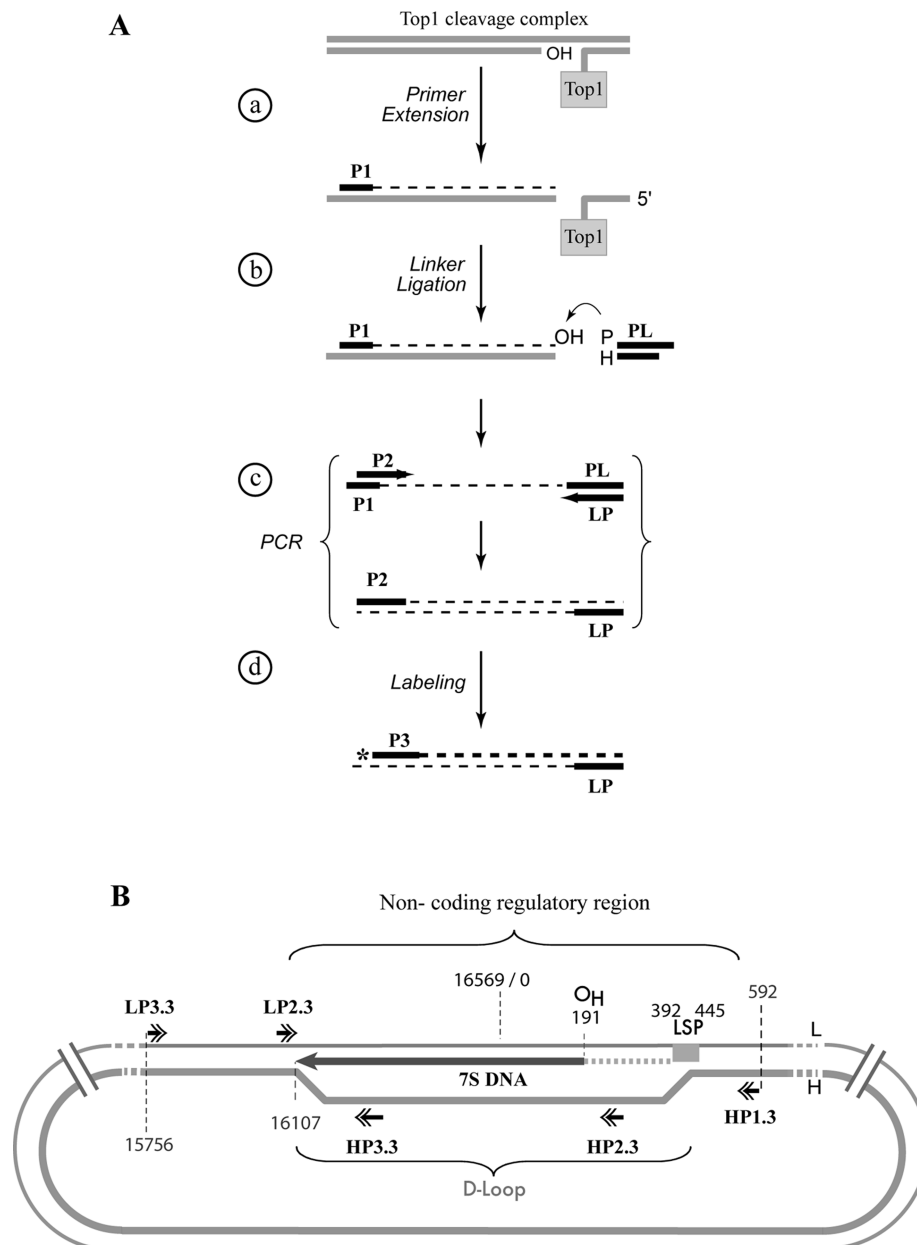
FIGURE 3: Experimental flowchart summarizing the experimental design for mapping Top1mt-induced cleavage sites in the mtDNA regulatory region. (A) Schematic representation of the PL-PCR protocol. (a) Primer extension was used to copy the broken strand (26, 27). (b) A universal primer (PL, phosphate linker) was ligated to the end of the extended strand. This linker has a phosphate at the 5′ end (P) and a dideoxynucleoside at the 3′ end (H) of the complementary strand to prevent unwanted ligation. (c) PCR with a nested P2 primer and a linker primer (LP) complementary to PL. (d) Labeling using a nested primer (P3) labeled at the 5′ end with ³²P (asterisk). (B) Schematic representation of the mtDNA noncoding regulatory region. The normally arrested D-loop (7S DNA) is represented with its termination at position 16107. Primers used for the PL-PCR are indicated with double arrowheads (see Table 2 for genomic positions and sequence): L, light strand; H, heavy strand; O_H, replication origin for the heavy strand; LSP, light strand promoter. The dotted horizontal gray line corresponds to the RNA primer from which the D-loop is initiated.

complexes but was less potent than CPT (Figure 2B). Low levels Top1mt−mtDNA cleavage complexes were also consistently detected in the absence of drug at 37 °C (the condition used for drug treatments) (Figure 2B, bottom left), whereas no detectable Top1 cleavage complexes were visible when mitochondria were kept at 0 °C (Figure 2B, top left). These results suggest that Top1mt−mtDNA cleavage complexes may form spontaneously. When mitochondria from different human cell lines, HCT116 colorectal carcinoma cells, and Jurkat leukemia T cells were used, CPT also trapped Top1mt−mtDNA cleavage complexes (data not shown). As the immunoassays above demonstrated the presence of Top1mt−mtDNA complexes, which presumably

corresponded to cleavage complexes, we designed experiments to map Top1mt cleavage sites in mtDNA.

In Organello Cleavage Sites of Top1mt in mtDNA. As Top1 forms cleavage complexes, it binds covalently to the DNA 3′ end and generates a free hydroxyl group at the 5′ end of the DNA break (20) (see the scheme at the top of Figure 3). To map the cleavage sites induced by Top1mt in mtDNA, we modified the ligation-mediated polymerase chain reaction (LM-PCR) approach (26, 27) by adding a phosphate group at the 5′ end of the linker (Figure 3b), so that the linker could be ligated to the 3′-OH group of the newly extended DNA strand (Figure 3a). To further increase the signal to noise ratio, we employed a dideoxynucleotide (ddNTP) at
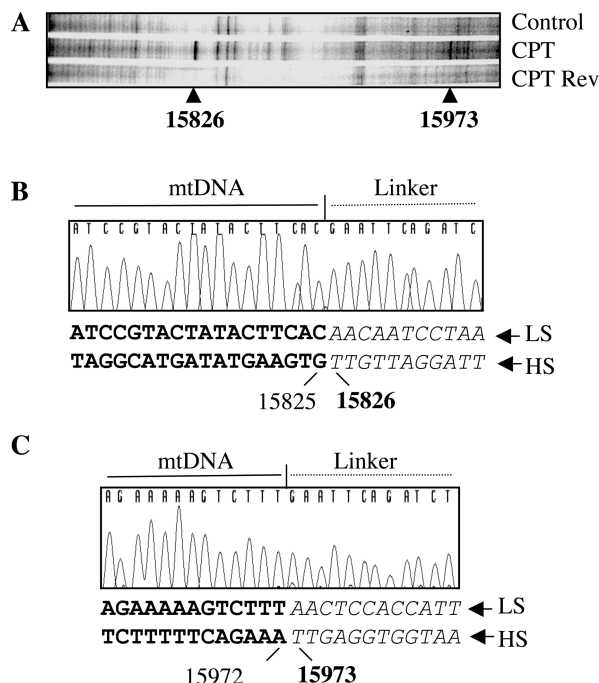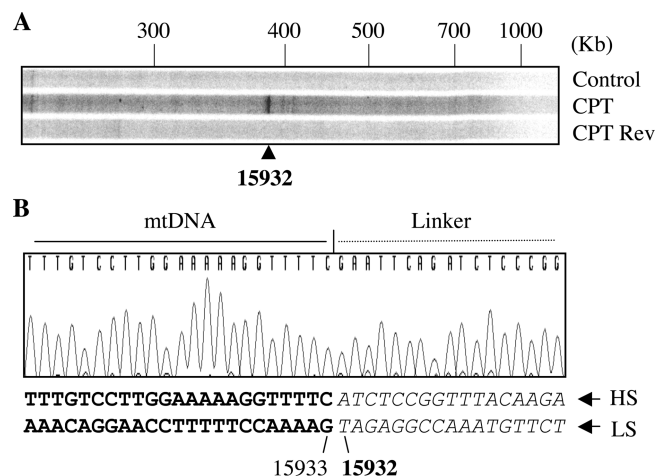
FIGURE 4: Mapping of Top1mt sites on the heavy strand of the mtDNA regulatory region. (A) PL-PCR result. The arrowheads indicate the Top1mt sites, and numbers correspond to their location in mtDNA. (B) Identification by sequencing of the corresponding DNA fragment obtained by PL-PCR for site 15826. The sequences of chromatograms show the mtDNA−linker junctions in the corresponding DNA fragments. The double-stranded sequences under each chromatogram show the corresponding mtDNA sequences. The boldface letters indicate the sequence portions presented in the chromatograms, and the italic letters represent the portions missing from the chromatograms. The numbers indicate the positions in mtDNA. Boldface numbers linked to the italic sequences are the sites where Top1mt was covalently linked to mtDNA: LS, light strand mtDNA; HS, heavy strand mtDNA. (C) Same for site 15973.

FIGURE 5: Mapping of Top1mt sites on the light strand of the mtDNA regulatory region. (A) PL-PCR result. The arrowhead indicates the Top1mt site. (B) Identification by sequencing of the corresponding DNA fragment obtained by PL-PCR. The sequence of the chromatogram shows the mtDNA−linker junction in the corresponding DNA fragment. The double-stranded sequence under the chromatogram shows the corresponding mtDNA sequence. The boldface letters indicate the sequence portion presented in the chromatogram, and the italic letters represent the portion missing from the chromatogram. The numbers indicate the positions in mtDNA. The boldface number linked to the italic sequence is the site where Top1mt covalently linked to mtDNA: LS, light strand mtDNA; HS, heavy strand mtDNA.

Table 2: Oligonucleotides for Mapping Top1mt Sites (see Figure 6)

L-15826	5′-TACTATACTTCACAACAATCCTAATC
H-15826	5′-GATTAGGATTGTTGTGAAGTATAGTA
L-15932	5′-GTAAACCGGAGATGAAAACCTTTTTC
H-15932	5′-GAAAAAGGTTTTCATCTCCGGTTTAC
L-15973	5′-AGAAAAAGTCTTTAACTCCACCATTA
H-15973	5′-TAATGGTGGAGTTAAAGACTTTTTCT

the 3′ end of the complementary strand of the linker (Figure 3b; denoted as "H"). We refer to this protocol as PL-PCR for phosphate linker, ligation-mediated PCR. Cycles of PCR were performed using a nested P2 primer and a primer (LP) complementary to the primer linker (PL) (Figure 3c). The broken DNA strands were labeled by primer extension with a third primer (P3; Figure 3d) labeled at the 5′ end with ^{32}P.

Figures 4 and 5 show representative experiments for Top1mt-induced cleavage sites in isolated mitochondria. We selected five primer sets (P1, P2, and P3 for each set; see Tables 1 and 2) to cover the regulatory D-loop region (Figure 3B). PL-PCR experiments showed a cluster of three sites consistently induced by CPT (Figures 4 and 5). Sequencing demonstrated their location at H15826, H15973 (Figure 4), and L15932 (Figure 5). Cleavage at those sites could be reversed by heat, a characteristic of Top1 cleavage complexes (28, 29). These experiments demonstrated the presence of Top1mt cleavage complexes in mtDNA, and their selective location in the regulatory region of mtDNA.

DNA Cleavage Sites Induced by Recombinant Top1mt in DNA Oligonucleotides Corresponding to the Sequences Cleaved in Mitochondria. To determine whether Top1mt-induced cleavage at the three sites of the mtDNA regulatory region was determined by the local DNA sequence, three 26mer duplex oligonucleotides corresponding to the Top1mt sites shown in Figures 4 and 5 were designed [H-15826,

L-15932, and H-15973 (Table 2)]. The potential cleavage sites previously observed in mtDNA were positioned in the center of the oligonucleotides to generate 13-mer cleavage products. Oligonucleotides H-15826, L-15932, and H-15973 were labeled at the 3′ end with [α-^{32}P]cordycepin and annealed to their corresponding complementary oligonucleotides, as Top1 requires duplex DNA for cleavage. Figure 6 shows that Top1mt cleaved the oligonucleotides at the same sites as in mitochondria. Cleavage efficiency was best for the H-15826 site and was relatively weak for the H15973 site. The difference in cleavage intensity may reflect an impact of mtDNA structure in vivo for optimal Top1mt activity.

Cleavage Sites Induced by Recombinant Top1mt in mtDNA in Vitro. To further determine the effect of local mtDNA structure on Top1mt activity, cleavage assays were carried out with long mtDNA fragments corresponding to the regions mapped in mitochondria. Those DNA fragments were obtained by PCR (see Figure 8B and Table 3) and were incubated with recombinant Top1mt. When the fragment encompassing to the H15826 and H15973 region was used, different patterns of cleavage sites were observed in vitro and in mitochondria (Figure 7). The H15973 site observed in mitochondria was not observed in vitro, which is consistent with the weak cleavage observed with the oligonucleotide centered by that site (see Figure 6). A new site, H15829, was observed in mtDNA in vitro. Additional experiments
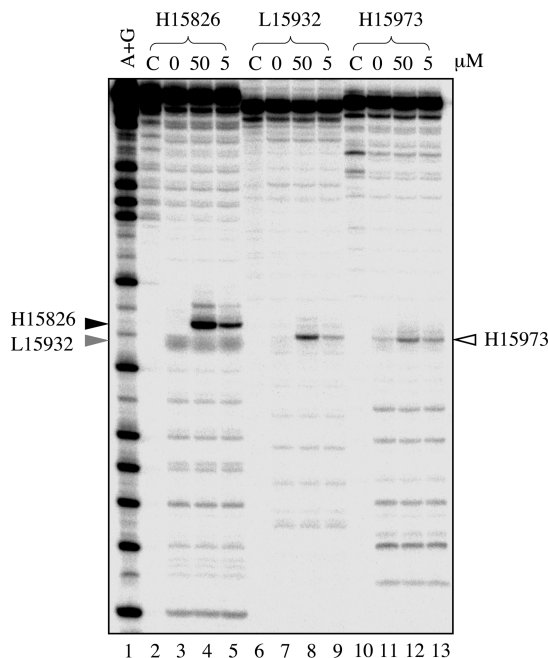
FIGURE 6: Top1mt sites in DNA oligonucleotides. Purified Top1mt was reacted with the indicated ³²P 3′-end-labeled oligonucleotides for 10 min at 37 °C. The oligonucleotide sequences are listed in Table 2. Arrowheads point to the Top1mt cleavage sites.

Table 3: Primers for Mapping Top1mt Sites in Vitro (see Figure 7)

Bam15741	GCGGATCCTCATTCTAACCTGAATC
Bam16249	GCGGATCCAAAGCCACCCCTCACC
Bam1611R	GCGGAACCGTACAATATTCATGGTGG
Bam-end	GCGGATCCATCGTGATGTCTTATTTAAG

were performed to scan both mtDNA strands in the region from residue 15741 to 16569 in vitro (see Figure 8B). We identified Top1mt sites that were spread along the isolated mtDNA but which had not been detectable in the experiments with mitochondria (Figure 8B). The differences in Top1mt cleavage pattern in organello and with isolated mtDNA suggest that mtDNA packaging regulates the cleavage sites induced by Top1mt in intact mitochondria.

Regulation of 7S DNA by Top1mt. The selective distribution of Top1mt sites ahead of the D-loop region in mtDNA suggested the possibility that Top1mt might play a role in regulating the premature termination of mtDNA replication that gives rise to the D-loop. Although the premature termination has been mapped to highly specific sites (*8, 9*), the molecular factors that control premature termination remain unknown. Using our PL-PCR assay (see steps b–d in Figure 3), we mapped the normal mouse mtDNA premature termination site at H15426 (*9*) (Figure 9).

Figure 9 shows that CPT reduced the level of formation of 7S DNA by approximately 50% [54 ± 10% in mitochondria from wild-type Top1mt⁺/⁺ MEF cells treated with CPT]. Similar experiments performed in mitochondria from Top1mt⁻/⁻ MEF cells showed a lack of an effect of CPT. Those results indicate that blocking Top1mt activity reduces the extent of D-loop formation in mitochondria and suggest the possibility that Top1mt acts as a DNA swivel to allow replication fork progression (*12–14*).

DISCUSSION

This study provides the first direct evidence of the presence of native Top1mt in mitochondria (see Figure 1), for its
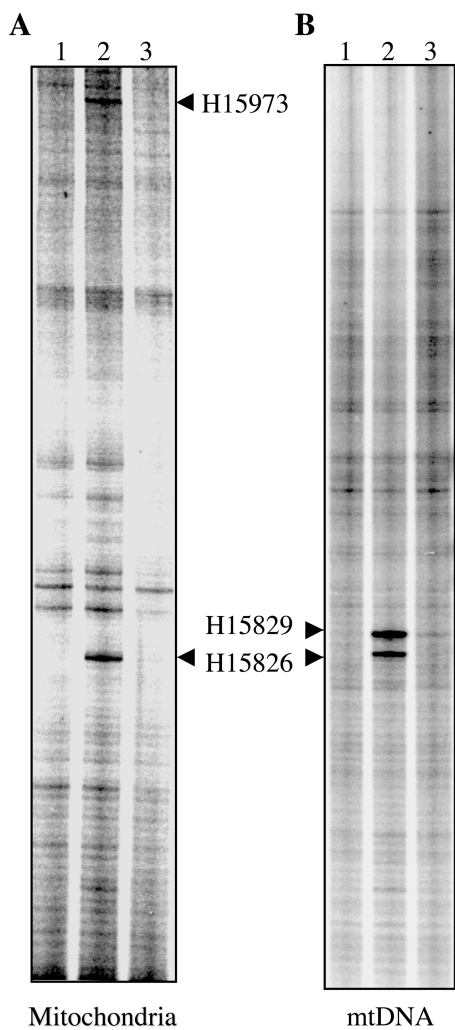

FIGURE 7: Comparison of Top1mt sites induced by CPT in mitochondria and with purified mtDNA and recombinant Top1mt. (A) Top1mt cleavage sites in mitochondria. (B) Top1mt cleavage sites in vitro. Arrowheads point to the Top1mt sites: lane 1, DNA alone; lane 2, DNA with CPT (50 μM); lane 3, DNA with CPT with heat reversal (65 °C for 5 min).

association with mtDNA (see Figures 2, 4, 5, and 7), of the nonrandom formation of Top1mt cleavage complexes in mtDNA in organello (Figures 4, 5, 7, and 8), and of a role for Top1mt in 7S DNA formation associated with the mtDNA D-loop.

Although Top1 activity can be readily detected from mitochondria from various sources (*15*), the biochemical isolation of the enzyme from mitochondria remained elusive until recently. Proteomic analyses published this year confirmed the presence of Top1mt in mitochondrial nucleoids (*30*). The difficulty in purifying mitochondrial topoisomerases is probably related to the small amount of enzymes present in mitochondria and to their limited and reversible association with mitochondrial nucleoids (*30*). This study provides four lines of evidence demonstrating the presence of Top1mt in mitochondria. First, immunoblotting of mitochondrial lysates with our Top1mt antibodies revealed the presence of an immunoreactive band migrating with the expected size range for Top1mt (Figure 1). Second, immunoblotting of mtDNA isolated with a cesium chloride gradient from mitochondria treated with CPT showed Top1mt tightly bound to mtDNA (Figure 2). Third, CPT-induced cleavage sites in mtDNA were demonstrated in mitochondria, and those sites coincided
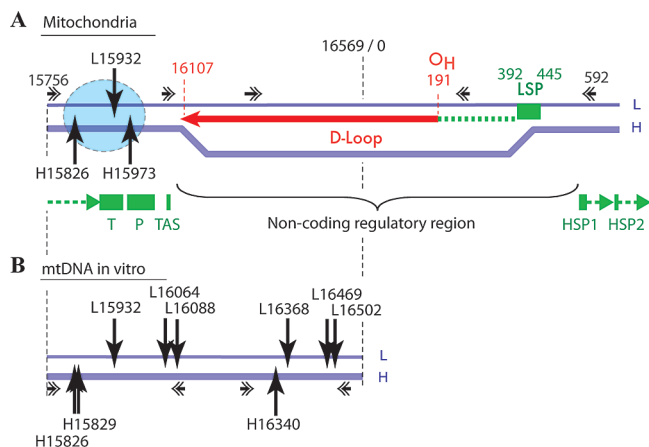
FIGURE 8: Mapping of the Top1mt sites in the regulatory D-loop region of mtDNA. (A) Top1mt sites in organello are clustered (light blue circle) downstream from the D-loop. (B) Top1mt sites in purified mtDNA are more widely distributed compared to the in organello sites. Primer sets used for the PL-PCR in mitochondria and primer used on mtDNA are indicated with a horizontal arrow with a double arrowhead. Top1mt sites are indicated by a vertical arrowhead pointing down for cleavage in the heavy (H) and light (L) strand. O_H denotes the origin of replication for the H-strand. The red arrow depicts the 7S DNA forming the D-loop and resulting from replication pausing at site 16107. LSP denotes the light strand promoter, which also serves as the RNA primer for H-strand synthesis. HSP1 and HSP2 denote H-strand promoters 1 and 2, respectively. T and P denote tRNAs for threonine and proline, respectively. TAS denotes the termination-associated sequence implicated in replication elongation arrest and D-loop formation (www.mitomap.org).
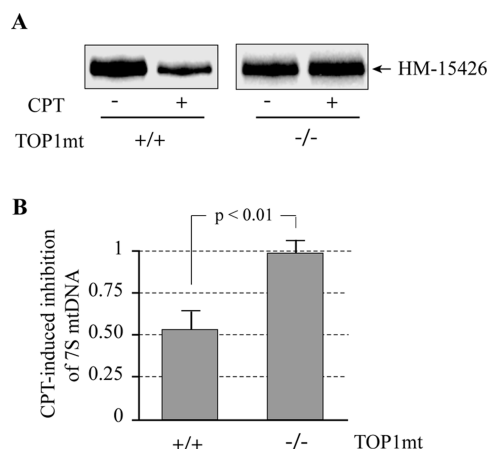
FIGURE 9: Inhibition of Top1mt by camptothecin (CPT) reduces the level of formation of 7S DNA. (A) Representative experiments in normal [Top1mt$^{+/+}$] and Top1mt-deficient [Top1mt$^{-/-}$] MEF mitochondria treated with CPT (as indicated; 50 μM at 37 °C for 30 min). (B) Top1mt-dependent inhibition of 7S DNA by CPT (50 μM at 37 °C for 30 min). Mean ± standard deviation (at least three independent experiments).

with cleavage sites induced by recombinant Top1mt in pure mtDNA (Figures 28). Fourth, treatment of mitochondria with CPT reduced the levels of 7S DNA, which was dependent upon the presence of Top1mt (Figure 9).

The need to generate specific anti-Top1mt antibodies to detect protein−DNA complexes was prompted by our finding that the existing antibodies against Top1 (nuclear) failed to cross-react against Top1mt. The lack of detectable cross-reactivity of the anti-Top1 polyclonal antibodies against Top1mt was surprising as the identity scores for the core, linker, and C-terminal domains of Top1 and Top1mt

polypeptides are high (73, 53, and 75%, respectively) (*15, 20*). Thus, it is possible that the titer of the available Top1 polyclonal antibodies tested was too low for detection of the normally weak Top1mt signal. The C21 monoclonal antibody, raised against the C-terminal peptide of nuclear Top1, also failed to detect Top1mt, which might reflect the existence of different epitopes of Top1mt in this region because five of 15 amino acids are different (K/R)-F-A-W-A-(I/L)-(D/A)-M-A-(D/G)-E-D-(Y/F)-E-F (Top1/Top1mt). It is also clear that our rabbit polyclonal antibodies generated against recombinant Top1mt are cross-reactive against (nuclear) Top1 (see Figure 1). Nevertheless, having generated antibodies that could react with Top1mt enabled us to demonstrate the induction of Top1−DNA complexes by CPT and the indenoisoquinoline Top1 inhibitor, MJ-III-65 (*14, 29*).

The induction of Top1mt−DNA complexes by CPT and MJ-III-65 (NSC706744) (*14*) demonstrates the functional association of Top1mt with mtDNA in organello. Indeed, Top1 must be engaged in its normal nicking−closing cycle to be trapped by drugs in cleavage complexes (*14, 22*). We detected the formation of cleavage complexes in mtDNA by immunoblotting mtDNA isolated from mitochondria with the Top1mt antibodies (see Figure 2). We also mapped the Top1mt cleavage complexes as cleavage sites in mtDNA using a variation of the LM-PCR assay we had previously used for mapping Top1 cleavage sites in rDNA (*26, 27*). We refer to the assay as PL-PCR (see Figure 3). Mapping of Top1mt sites in the regulatory 1.3 kb region spanning the regulatory region of mtDNA in organello revealed only three detectable sites clustered within a 150 bp region downstream from the D-loop (summarized in Figure 8A). By contrast, mapping of Top1mt sites in a 0.7 kb overlapping segment in purified mtDNA revealed nine sites distributed throughout both strands of the mtDNA, including in the D-loop region (see Figure 8B). Two of the in organello sites were exactly at the same location in purified mtDNA (H15826 and L15932). Only one site (H15973) could be detected in organello but not in purified mtDNA. However, that site (H15973) was detectable, albeit only weakly in an oligonucleotide in the presence of recombinant Top1mt (Figure 6). The sequestration of the Top1mt sites next to the end of the D-loop in the mitochondrial regulatory region suggests that the mitochondrial nucleoid structure (*30*) directs the accessibility of mtDNA to Top1mt.

The D-loop is a segment of the mitochondrial genome defined by the presence of a displacement loop, which has been attributed to the pausing of DNA polymerase γ around position 16100 (*8*) (see Figure 8). Using the modified PL-PCR technique (see Materials and Methods), we mapped the 3′ end of human 7S DNA at position 16107 in breast cancer MCF-7 cells, which agrees with previous data reporting position 16106 (*8*). However, in mouse cells, we found a prominent 7S DNA 3′ end at position 15426 instead of multiple sites around that same region (*8*). This difference may reflect either the difference in methods or the difference in the mtDNA structure in various mitochondrial preparations. Our findings that 7S DNA was reduced by CPT in a Top1mt-dependent manner (see Figure 9) along with the clustering of Top1mt sites downstream from the 3′ end of the D-loop show that Top1mt may play a role in D-loop homeostasis. The effect of CPT on the D-loop could be due

to replication and/or transcription alterations and other DNA-related functions in response to the poisoning of Top1mt.

REFERENCES

1. Schapira, A. H. (2006) Mitochondrial disease. *Lancet 368*, 70–82.
2. Kang, D., and Hamasaki, N. (2005) Alterations of mitochondrial DNA in common diseases and disease states: Aging, neurodegeneration, heart failure, diabetes, and cancer. *Curr. Med. Chem. 12*, 429–441.
3. Dimauro, S., and Davidzon, G. (2005) Mitochondrial DNA and disease. *Ann. Med. 37*, 222–232.
4. Wallace, D. C. (2005) A mitochondrial paradigm of metabolic and degenerative diseases, aging, and cancer: A dawn for evolutionary medicine. *Annu. Rev. Genet. 39*, 359–407.
5. Chen, X. J., and Butow, R. A. (2005) The organization and inheritance of the mitochondrial genome. *Nat. Rev. Genet. 6*, 815–825.
6. Shadel, G. S., and Clayton, D. A. (1997) Mitochondrial DNA maintenance in vertebrates. *Annu. Rev. Biochem. 66*, 409–435.
7. Bonawitz, N. D., Clayton, D. A., and Shadel, G. S. (2006) Initiation and beyond: Multiple functions of the human mitochondrial transcription machinery. *Mol. Cell 24*, 813–825.
8. Doda, J. N., Wright, C. T., and Clayton, D. A. (1981) Elongation of displacement-loop strands in human and mouse mitochondrial DNA is arrested near specific template sequences. *Proc. Natl. Acad. Sci. U.S.A. 78*, 6116–6120.
9. Fish, J., Raule, N., and Attardi, G. (2004) Discovery of a major D-loop replication origin reveals two modes of human mtDNA synthesis. *Science 306*, 2098–2101.
10. Garrido, N., Griparic, L., Jokitalo, E., Wartiovaara, J., van der Bliek, A. M., and Spelbrink, J. N. (2003) Composition and dynamics of human mitochondrial nucleoids. *Mol. Biol. Cell 14*, 1583–1596.
11. Albring, M., Griffith, J., and Attardi, G. (1977) Association of a protein structure of probable membrane derivation with HeLa cell mitochondrial DNA near its origin of replication. *Proc. Natl. Acad. Sci. U.S.A. 74*, 1348–1352.
12. Wang, J. C. (2002) Cellular roles of DNA topoisomerases: A molecular perspective. *Nat. Rev. Mol. Cell Biol. 3*, 430–440.
13. Champoux, J. J. (2001) DNA topoisomerases: Structure, function, and mechanism. *Annu. Rev. Biochem. 70*, 369–413.
14. Pommier, Y. (2006) Topoisomerase I inhibitors: Camptothecins and beyond. *Nat. Rev. Cancer 6*, 789–802.
15. Zhang, H., Meng, L. H., and Pommier, Y. (2007) Mitochondrial topoisomerases and alternative splicing of the human TOP1mt gene. *Biochimie 89*, 474–481.
16. Corbett, K. D., and Berger, J. M. (2004) Structure, molecular mechanisms, and evolutionary relationships in DNA topoisomerases. *Annu. Rev. Biophys. Biomol. Struct. 33*, 95–118.
17. Castora, F. J., and Lazarus, G. M. (1984) Isolation of a mitochondrial DNA topoisomerase from human leukemia cells. *Biochem. Biophys. Res. Commun. 121*, 77–86.
18. Lin, J. H., and Castora, F. J. (1995) Response of purified mitochondrial DNA topoisomerase I from bovine liver to camptothecin and m-AMSA. *Arch. Biochem. Biophys. 324*, 293–299.
19. Kosovsky, M. J., and Soslau, G. (1991) Mitochondrial DNA topoisomerase I from human platelets. *Biochim. Biophys. Acta 1078*, 56–62.
20. Zhang, H., Barcelo, J. M., Lee, B., Kohlhagen, G., Zimonjic, D. B., Popescu, N. C., and Pommier, Y. (2001) Human mitochondrial topoisomerase I. *Proc. Natl. Acad. Sci. U.S.A. 98*, 10608–10613.
21. Zhang, H., Meng, L. H., Zimonjic, D. B., Popescu, N. C., and Pommier, Y. (2004) Thirteen-exon-motif signature for vertebrate nuclear and mitochondrial type IB topoisomerases. *Nucleic Acids Res. 32*, 2087–2092.
22. Hsiang, Y. H., Hertzberg, R., Hecht, S., and Liu, L. F. (1985) Camptothecin induces protein-linked DNA breaks via mammalian DNA topoisomerase I. *J. Biol. Chem. 260*, 14873–14878.
23. Bogenhagen, D., and Clayton, D. A. (1974) The number of mitochondrial deoxyribonucleic acid genomes in mouse L and human HeLa cells. Quantitative isolation of mitochondrial deoxyribonucleic acid. *J. Biol. Chem. 249*, 7991–7995.
24. Subramanian, D., Kraut, E., Staubus, A., Young, D. C., and Muller, M. T. (1995) Analysis of topoisomerase I/DNA complexes in patients administered topotecan. *Cancer Res. 55*, 2097–2103.
25. Pourquier, P., Takebayashi, Y., Urasaki, Y., Gioffre, C., Kohlhagen, G., and Pommier, Y. (2000) Induction of topoisomerase I cleavage complexes by 1-β-D-arabinofuranosylcytosine (Ara-C) *in vitro* and in ara-C-treated cells. *Proc. Natl. Acad. Sci. U.S.A. 97*, 1885–1890.
26. Strumberg, D., Pilon, A. A., Smith, M., Hickey, R., Malkas, L., and Pommier, Y. (2000) Conversion of topoisomerase I cleavage complexes on the leading strand of ribosomal DNA into 5′-phosphorylated DNA double-strand breaks by replication runoff. *Mol. Cell. Biol. 20*, 3977–3987.
27. Pondarre, C., Strumberg, D., Fujimori, A., Torres-Leon, R., and Pommier, Y. (1997) In vivo sequencing of camptothecin-induced topoisomerase I cleavage sites in human colon carcinoma cells. *Nucleic Acids Res. 25*, 4111–4116.
28. Hsiang, Y. H., and Liu, L. F. (1988) Identification of mammalian DNA topoisomerase I as an intracellular target of the anticancer drug camptothecin. *Cancer Res. 48*, 1722–1726.
29. Antony, S., Jayaraman, M., Laco, G., Kohlhagen, G., Kohn, K. W., Cushman, M., and Pommier, Y. (2003) Differential induction of topoisomerase I-DNA cleavage complexes by the indenoisoquinoline MJ-III-65 (NSC 706744) and camptothecin: Base sequence analysis and activity against camptothecin-resistant topoisomerases I. *Cancer Res. 63*, 7428–7435.
30. Bogenhagen, D. F., Rousseau, D., and Burke, S. (2008) The Layered Structure of Human Mitochondrial DNA Nucleoids. *J. Biol. Chem. 283*, 3665–3675.

BI800774B